Published in final edited form as:
Neurobiol Aging. 2014 January ; 35(1): . doi:10.1016/j.neurobiolaging.2013.07.007.

L-type Ca^{2+} currents at CA1 synapses, but not CA3 or dentate granule neuron synapses, are increased in 3xTgAD mice in an age-dependent manner

Yue Wang[a,*] and **Mark P. Mattson**[a,b]

[a]Laboratory of Neurosciences, National Institute on Aging Intramural Research Program, Baltimore, MD, USA

[b]Department of Neuroscience, Johns Hopkins University School of Medicine, Baltimore, MD, USA

Abstract

Abnormal neuronal excitability and impaired synaptic plasticity might occur before the degeneration and death of neurons in Alzheimer's disease (AD). To elucidate potential biophysical alterations underlying aberrant neuronal network activity in AD, we performed whole-cell patch clamp analyses of L-type (nifedipine-sensitive) Ca^{2+} currents (L-VGCC), 4–aminopyridine-sensitive K^+ currents, and AMPA (2-amino-3-(3-hydroxy-5-methyl-isoxazol-4-yl)propanoic acid) and NMDA (N-methyl-D-aspartate) currents in CA1, CA3, and dentate granule neurons in hippocampal slices from young, middle-age, and old 3xTgAD mice and age-matched wild type mice. 3xTgAD mice develop progressive widespread accumulation of amyloid b-peptide, and selective hyperphosphorylated tau pathology in hippocampal CA1 neurons, which are associated with cognitive deficits, but independent of overt neuronal degeneration. An age-related elevation of L-type Ca^{2+} channel current density occurred in CA1 neurons in 3xTgAD mice, but not in wild type mice, with the magnitude being significantly greater in older 3xTgAD mice. The NMDA current was also significantly elevated in CA1 neurons of old 3xTgAD mice compared with in old wild type mice. There were no differences in the amplitude of K^+ or AMPA currents in CA1 neurons of 3xTgAD mice compared with wild type mice at any age. There were no significant differences in Ca^{2+}, K^+, AMPA, or NMDA currents in CA3 and dentate neurons from 3xTgAD mice compared with wild type mice at any age. Our results reveal an age-related increase of L-VGCC density in CA1 neurons, but not in CA3 or dentate granule neurons, of 3xTgAD mice. These findings suggest a potential contribution of altered L-VGCC to the selective vulnerability of CA1 neurons to tau pathology in the 3xTgAD mice and to their degeneration in AD patients.

Keywords

3xTgAD mice; Aging; L-type Ca^{2+} currents; CA1

[*]Corresponding author at: National Institute on Aging Intramural Research Program, Department of Neurosciences, Baltimore, MD 21224-6825, USA. Tel.: 410 558 8462; fax: 410 558 8465., wangyu@grc.nia.nih.gov (Y. Wang). .

Disclosure statement

The authors have no competing financial interests.

All experiments complied with National Institutes of Health guidelines and were approved by the National Institute on Aging Animal Care and Use Committee.

Appendix A. Supplementary data

Supplementary data associated with this article can be found, in the online version, at http://dx.doi.org/10.1016/j.neurobiolaging.2013.07.007.

1. Introduction

Multiple lines of evidence suggest an important role for disturbed cellular Ca^{2+} regulation in the selective vulnerability of neurons in Alzheimer's disease (AD). Studies of postmortem brain tissue samples revealed hyperactivation of Ca^{2+}-dependent proteases in degenerating neurons of AD patients compared with those in age-matched control subjects (Saito et al., 1993). Exposure of cultured human cortical neurons to amyloid-β peptide (Aβ) results in abnormally large elevations of intracellular Ca^{2+} levels in response to activation of glutamate receptors, thereby rendering the neurons vulnerable to excitotoxicity (Mattson et al., 1992). The latter findings are consistent with evidence that seizures are common in AD patients (Gleichmann et al., 2011; Larner, 2011), and data from studies of transgenic mice that accumulate Aβ deposits in their brains in which intracellular Ca^{2+} levels are elevated in neurites associated with the Aβ (Kuchibhotla et al., 2008). Aβ might compromise neuronal Ca^{2+} homeostasis by causing membrane-associated oxidative stress which impairs the function of the Na^+/K^+-ATPase, Ca^{2+}-ATPase, and glucose transporter GLUT3 (glutamate transporter 3) (Mark et al., 1995, 1997), and by causing hyperactivation of Ca^{2+}-dependent enzymes (Wu et al., 2010). Neurons can be protected from being damaged by Aβ using several treatments that reduce Ca^{2+} influx including agents that block voltage-dependent Ca^{2+} channels (Anekonda and Quinn, 2011;Yagami et al., 2004), glutamate receptors (Mattson et al., 1992), and ryanodine receptor channels (Guo et al., 1997; Oulès et al., 2012; Peng et al., 2012).

Mutations in presenilin-1, the enzymatic component of the γ-secretase complex that cleaves the Aβb precursor protein resulting in the release of Aβ, account for a large number of cases of early-onset inherited AD (Schellenberg and Montine, 2012). In addition to their role in Aβ generation, presenilin-1 mutations can cause excessive release of Ca^{2+} from the endoplasmic reticulum (ER) (via ryanodine and IP_3 [inositol triphosphate] receptor channels) which can impair synaptic plasticity and sensitize neurons to excitotoxicity in an Aβ-independent manner (Chakroborty et al., 2012; Guo et al., 1999; Ito et al., 1994). Tau pathology has also been associated with altered Ca^{2+} regulation. For example, when expressed in cultured neurons, mutations in tau that cause accumulation of hyperphosphorylated tau (p-tau) in frontotemporal lobe dementia destabilize cellular Ca^{2+} homeostasis (Furukawa et al., 2003). On the other hand, excessive elevation of Ca^{2+} levels in neurons can promote accumulation of p-tau and microtubule depolymerization similar to that which occurs in vulnerable neurons in AD (Flaherty et al., 2000; Mattson, 1990; Medeiros et al., 2012).

Advancing age is the major risk factor for the most common late-onset cases of AD (Kawas and Corrada, 2006). Electrophysiological analyses of ion channels in hippocampal CA1 neurons of rats have demonstrated an age-related increase in L-type voltage-gated Ca^{2+} currents (L-VGCC) (Disterhoft et al., 2004; Landfield, 1994). Further analysis showed that the activity of single L-type channels in CA1 neurons is increased with aging (Thibault and Landfield, 1996). However, it is not known whether an age-related increase in Ca^{2+} currents is specific for CA1 neurons or also occurs in CA3 pyramidal neurons and dentate granule neurons. The latter question is of considerable interest because CA1 neurons are selectively vulnerable to degeneration in AD, whereas CA3 neurons are less vulnerable and dentate granule neurons do not degenerate (Mattson and Magnus, 2006; Simonian and Hyman, 1995). Because CA1 neurons are more prone to accumulating p-tau and neurofibrillary tangles, it is also important to know whether p-tau is associated with elevated L-type Ca^{2+} currents. To address these questions we recorded whole-cell Ca^{2+}, K^+, AMPA (2-amino-3-(3-hydroxy-5-methyl-isoxazol-4-yl) propanoic acid) and NMDA (N-methyl-D-aspartate) currents in CA1, CA3, and dentate granule neurons in hippocampal slices from young, middle-age, and old 3xTgAD and wild type (WT) mice. The 3xTgAD mice develop age-

related accumulation of Aβ throughout the hippocampus, and p-tau accumulates in CA1 neurons, but not in CA3 or granule neurons (Kashiwaya et al., 2013; Oddo et al., 2003).

In the present study, we found that the L-VGCC density is significantly elevated in CA1 neurons of old, but not younger 3xTgAD mice compared with age-matched WT mice. In contrast, the L-VGCC of CA3 pyramidal neurons and dentate granule neurons is normal throughout the life of the 3xTgAD mice. These findings suggest a hippocampal neuron subregion-selective association of elevated L-VGCC with p-tau pathology in 3xTgAD mice. If a similar alteration of L-VGCC occurs in AD, it might contribute to the selective vulnerability of CA1 neurons, and therapeutic interventions that normalize the L-VGCC has therapeutic potential.

2. Methods

2.1. Chemicals

Nifedipine, APV ((2R)-amino-5-phosphonovaleric acid; (2R)-amino-5-phosphonopentanoate), and NBQX (2,3-dihydroxy-6-nitro-7-sulfamoyl-benzo[f]quinoxaline-2,3-dione) were from Tocris Bioscience. Nifedipine was prepared as a 100-mM stock in DMSO (dimethylsulfoxide) and used at a final concentration of 30 μM in artificial cerebrospinal fluid (ACSF). D-AP5 was prepared as a 100-mM stock in Millipore water and used at a final concentration of 50 μM in ACSF. NBQX was prepared as a 20-mM stock in DMSO, and used at a final concentration of 10 μM in ACSF.

2.2. Animals

3xTgAD mice (Oddo et al., 2003), that had been backcrossed to C57BL/6 mice for 8 generations (Kashiwaya et al., 2013; Liu et al., 2010), and nontransgenic control C57BL/6 mice ranging in age from 1 to 26 months were used in this study. All experiments complied with National Institutes of Health guidelines and were approved by the National Institute on Aging Animal Care and Use Committee.

2.3. Electrophysiology

Hippocampal slices were prepared using procedures described previously (Wang et al., 2009). Briefly, the mice were euthanized with isoflurane, their brains were rapidly removed, and transverse slices of the hippocampus were cut at a thickness of 350 μm. The slices were allowed to recover for at least 1 hour in ACSF at room temperature before recording. ACSF consisted of: 120 mM NaCl, 2.5 mM KCl,1.25 mM NaH_2PO_4, 26 mM $NaHCO_3$,1.3 mM $MgSO_4$, 2.5 mM $CaCl_2$, and 10 mM glucose (pH 7.4). The osmolarity of the ACSF was adjusted to 290 mmol/kg using a 5520 Vapor Pressure Osmometer (Wescor, Inc). All recordings were performed at 30 °C–32 °C.

For whole-cell excitatory postsynaptic current recordings from CA1 and CA3 pyramidal neurons and dentate granule cells, the neurons were visualized using differential interference contrast microscopy and a 40× water immersion lens. For recordings of L-VGCC and IA (A-type potassium channel current), the ACSF contained: 95 mM NaCl, 25 mM tetraethyl ammonium chloride, 2.5 mM KCl, 1.3 mM $MgSO_4$, 2 mM $CaCl_2$, 1 mM NaH_2PO_4, 26 mM $NaHCO_3$, and 10 mM glucose (Kochlamazashvili et al., 2010). Series resistance was 10–15 MΩ (data were discarded if the resistance varied by more than 10% during the recording period). The patch-clamp electrode (3–4 MΩ) internal solution contained $CsMeSO_3$, 2.5 mM CsCl, 8 mM NaCl, 7 mM tetraethyl ammonium, 20 mM HEPES (4-(2-hydroxyethyl)-1-piperazineethanesulfonic acid), 0.2 mM (ethylene glycol tetraacetic acid), 5 mM Mg ATP (adenosine triphosphate), 0.3 mM Na-GTP (guanosine triphosphate), and 5 mM QX 314 (pH 7.2, adjusted using CsOH), and 280–290 mmol/Kg (Zhang et al., 2011). A series of voltage

steps (100 ms) from −60 mV to 60 mV generated L-VGCC and a transient outward 4-aminopyridine (4-AP)-sensitive K^+ current as described previously (Connor and Stevens, 1971; Gustafsson et al., 1982; Kochlamazashvili et al., 2010). Sodium currents and synaptic transmission were blocked by adding 1 μM TTX (tetrodotoxin), 10 mM NBQX, 100 mM APV, and 100 μM picrotoxin to the extracellular solution. Series voltage steps (20 mV and 150 ms) from −70 mV to 40 mV generated AMPA and NMDAR (NMDA receptor) currents simultaneously (Zhang et al., 2011). To avoid capacitance transients generated by the step effect on the current, there was a delay of 50 ms between the start of a step and presynaptic stimulation. We routinely applied APV or NBQX to verify the amplitude of each current. In most cases, in presence of APV, the AMPA current increased by 5%–10%, consistent with reciprocal inhibition of these 2 types of ionotropic glutamate receptors (Gray et al., 2011; Lu et al., 2011; Schoppa et al., 1998). Data were collected using a MultiClamp 700B amplifier (Molecular Devices). Signals were filtered at 2 kHz and digitized at 10 kHz with a Digidata 1440A Data Acquisition System, and analyzed using pCLAMP 10 software (Molecular Devices). The Multiclamp 700B amplifier is designed to compensate series resistance. In addition, cesium was included in the internal patch solution, which previous studies have shown greatly reduces space-clamp errors (Schaefer et al., 2003; Stuart and Sakmann, 1994).

2.4. Data analysis

Data are presented as the mean ± standard error. Statistical significance was assessed using an unpaired 2-tailed Student *t* test or an analysis of variance test with Tukey-Kramer post hoc analysis.

3. Results

3.1. Age-dependent elevation of L-VGCC amplitude in CA1 pyramidal neurons of 3xTgAD mice

The congenic line of 3xTgAD mice used in this study exhibit no discernible p-tau or Aβ pathologies, and no cognitive deficits, before 6 months of age; thereafter, CA1 neurons accumulate p-tau and cognitive deficits occur (Halagappa et al., 2007). To determine whether the L-VGCC was altered in CA1 pyramidal neurons in 3xTgAD mice, we recorded L-VGCC in CA1 neurons in hippocampal slices from young (1-month-old), middle-age (6–9-month-old) and older (12–16-month-old) 3xTgAD and WT mice (Fig. 1). As expected, there was an age-related increase in the L-VGCC amplitude in WT mice, and this also occurred in 3xTgAD mice. There were no differences between WT and 3xTgAD mice in the L-VGCC amplitude in 1-month-old mice (300 ± 20.1 pA and 302 ± 19.6 pA, respectively) or in 6–9-month-old mice (312 ± 20.2 pA and 318 ± 22.3 pA, respectively). In contrast, the L-VGCC amplitude was significantly greater in CA1 neurons in slices from 12–16-month-old 3xTgAD mice (368 ± 18.9 pA) compared with age-matched WT mice (328 ± 19.6 pA) (Fig. 1B and C). The current–voltage relationship for L-type channel recordings are shown in Fig. 1D. We also determined the L-VGCC density as a function of age in CA1 neurons of WT and 3xTgAD mice. Previous studies have shown that an age-related increase in whole-cell L-VGCC that occurs in cultured hippocampal neurons results mainly from an increase in the L-VGCC current density (Porter et al., 1997). We found that, in agreement with the LVGCC amplitude data (Fig. 1C), the L-VGCC density was significantly greater in CA1 neurons of older (12–16-month-old) 3xTgAD mice compared with age-matched WT mice, whereas there was a significant difference in the L-VGCC density in CA1 neurons of younger 3xTgAD and WT mice (Fig. 1E).

3.2. L-VGCCs in CA3 pyramidal neurons and dentate granule neurons are unaffected by age and is not different in 3xTgAD and WT mice

To determine whether the enhancement of L-VGCC in CA1 neurons of older 3xTgAD mice was specific for CA1 neurons, we recorded L-VGCC in CA3 pyramidal neurons and dentate granule neurons in slices from young, middle-age, and older 3xTgAD and WT mice. There was no significant effect of age on L-VGCC amplitude in CA3 or dentate granule neurons in either WT or 3xTgAD mice (Fig. 2A and B). There were no significant differences in the CA3 neuron L-VGCC amplitudes in 3xTgAD mice compared with WT mice at any age (Fig. 2A). The current amplitudes were, for 1-month-old mice: WT, 289 ± 15.6 pA; 3xTgAD, 291 ± 20.2 pA; for 6–9-month-old mice: WT, 293 ± 19.5 pA; 3xTgAD, 294 ± 18.9 pA; and for 12–16-month-old mice: WT, 303 ± 21.2 pA; 3xTgAD, 316 ± 18.8 pA. There were no signi ficant differences in the dentate granule neuron L-VGCC amplitudes in 3xTgAD mice compared with WT mice at any age; for 1-month-old mice: WT, 288 ± 16.8 pA; 3xTgAD, 290 ± 20.5 pA; for 6–9-month-old mice: WT, 292 ± 18.5 pA; 3xTgAD, 295 ± 16.8 pA; and for 12–16-month-old mice: WT, 302 ± 17.2 pA; 3xTgAD, 315 ± 18.1 pA (Fig. 2B). Previous studies have shown that 4–AP-sensitive K channels are the predominant K^+ current in CA1 pyramidal neurons, + and play a critical role in the control of neuronal excitability and synaptic NMDA receptor function (Andrásfalvy et al., 2008; Storm, 1990). We first isolated the IA current and showed that, as expected, the current was inhibited by 4-AP (2 mM) (Fig. 3A). The 4–AP-sensitive current was unaffected by age in CA1, CA3, and dentate granule neurons of WT and 3xTgAD mice (Fig. 3A-C). In CA1 neurons, the K^+ currents were not significantly different in slices from WT and 3xTgAD mice at any age; 1-month-old mice: WT, 420 ± 32.1 pA; 3xTgAD, 415 ± 25.6 pA; 6–9-month-old mice: WT, 418 ± 30.2 pA; 3xTgAD, 422 ± 22.3 pA; and 12–16-month-old mice: WT, 425 ± 28.8 pA; 3xTgAD, 410 ± 29.9 pA (Fig. 3A; Supplementary Fig. 1A). The K^+ currents in CA3 neurons were not different in slices from WT and 3xTgAD mice; 1-month-old: WT, 420 ± 32.1 pA; 3xTgAD, 415 ± 24.6 pA; 6–9-month-old: WT, 425 ± 24.2 pA; 3xTgAD, 428 ± 22.3 pA; and 12–16-month-old: WT, 435 ± 24.8 pA; 3xTgAD, 438 ± 22.9 pA (Fig. 3B). The K^+ currents were also not different in dentate granule neurons in slices from WT and 3xTgAD mice; 1-month-old: WT, 398 ± 29.9 pA; 3xTgAD, 405 ± 25.6 pA; 6–9-month-old: WT, 388 ± 32.2 pA; 3xTgAD, 400 ± 28.3 pA; and 12–16-month-old: WT, 395 ± 28.8 pA; 3xTgAD, 398 ± 21.8 pA (Fig. 3C).

3.3. NMDA current amplitude in CA1 neurons is unaffected by aging and is modestly elevated in older 3xTgAD mice

Because excessive Ca^{2+} influx through NMDA receptors is implicated in the neurodegenerative process in AD (Goussakov et al., 2010; Landfield et al., 1989; Mattson et al., 1992; Shankar et al., 2007), we measured whole-cell NMDA and AMPA currents in CA1 neurons in hippocampal slices from WT and 3xTgAD mice. The AMPA current amplitude was unaffected by age and was not significantly different in slices from WT and 3xTgAD mice in any of the 3 age groups: 1-month-old (WT, 172 ± 13.12 pA; 3xTgAD, 168 ± 12.59 pA); 6–9-month-old (WT, 165 ± 14.22 pA; 3xTgAD, 166 ± 15.58 pA); and 12–16-month-old (WT, 168 ± 13.0 pA; 3xTgAD, 170 ± 14.1 pA) (Fig. 4A). The NMDA current amplitude was not different in young and middle-age 3xTgAD mice compared with age-matched WT mice (1-month-old, WT: 230 ± 15.2 pA; 3xTgAD, 228 ± 13.2 pA; 6–9-month-old, WT, 238 ± 16.4 pA; 3xTgAD, 235 ± 13.8 pA) (Fig. 4B). However, in the older 3xTgAD mice, the NMDA current amplitude and current density was significantly ($p < 0.05$), albeit modestly, elevated (250 ± 12.7 pA) compared with age-matched WT mice (230 ± 15.9 pA) (Fig. 4B; Supplementary Fig. 1B).

4. Discussion

Previous studies of rat hippocampal CA1 neurons during normal aging in rabbits and rats demonstrated increased L-type Ca^{2+} currents and an associated enhancement of Ca^{2+}-dependent after-hyperpolarizations (Campbell et al., 1996; Matthews et al., 2009; Moyer et al., 1992; Santos et al., 2010). In the present study, we did not detect an age-related increase of the L-VGCC in CA1 neurons of WT mice. However, because the main purpose of the present study was to compare currents in neurons in different hippocampal subfields of 3xTgAD and WT mice, we did not evaluate very old mice (older than the age of 16 months). We therefore cannot rule out the possibility that the L-VGCC density would increase after 16 months of age in WT mice; indeed, we did observe a trend for an age-related increase of the L-VGCC in CA1 neurons of WT mice. We found that the L-VGCC density in CA1 neurons of 12–16-month-old 3xTgAD mice was significantly greater than that in age-matched WT mice, whereas there was no difference in the L-VGCC density in younger 3xTgAD and WT mice. In contrast, we found that the 4–AP-sensitive current amplitude in CA1 neurons was remarkably stable during normal aging, and was unchanged in the 3xTgAD mouse model of AD. There were no significant effects of age or mouse genotype on L-VGCC in CA3 and dentate granule neurons. The whole-cell 4–AP-sensitive K^+ current amplitude did not change with age and was not different in 3xTgAD mice compared with in WT mice in CA1, CA3, or dentate neurons.

Findings from studies of AD patients and experimental models suggest that excessive Ca^{2+} influx and associated synaptic dysfunction occur in vulnerable neurons in AD (Mattson and Magnus, 2006; Sandin et al., 1990). However, the reason(s) why CA1 neurons are vulnerable to degeneration in AD, whereas CA3 neurons are less vulnerable and dentate granule neurons are resistant, is unknown. Our findings suggest 1 possible explanation for the selective vulnerability of CA1 neurons, namely, that they are prone to excessive Ca^{2+} influx through L-VGCC. Although the contribution of enhanced L-VGCC to the selective vulnerability of CA1 neurons in AD remains to be established, considerable data are consistent with its pivotal involvement. First, blockers of L-VGCC can protect neurons and preserve synaptic function in animal models of aging and AD (Anekonda and Quinn, 2011; Levere and Walker, 1992; Paris et al., 2011; Roberts-Lewis et al., 1994; Veng et al., 2003). Second, CA1 neurons are particularly prone to cellular Ca^{2+} overload and degeneration in conditions of impaired energy metabolism. For example, transient global ischemia results in the selective Ca^{2+}-mediated degeneration of CA1 neurons with the sparing of dentate granule neurons and CA3 neurons (Calderone et al., 2004; Roberts-Lewis et al., 1994). In addition, mitochondrial function is impaired in CA1 neurons in aging and AD (Cottrell et al., 2001; Yao et al., 2009), and sustaining cellular bioenergetic properties reduces p-tau pathology in CA1 neurons and ameliorates learning and memory deficits in 3xTgAD mice (Kashiwaya et al., 2013). Third, CA1 neurons are prone to p-tau/neurofibrillary pathology in AD patients (Arnold et al., 1991) and 3xTgAD mice (Oddo et al., 2003), and expression in hippocampal neurons of tau mutations that cause p-tau and neurofibrillary pathology result in increased L-VGCC amplitude and excessive Ca^{2+} influx (Furukawa et al., 2003). Because CA1 pyramidal neurons, but not CA3 or dentate granule neurons accumulate p-tau in 3xTgAD mice (Oddo et al., 2003), it is therefore possible that the p-tau pathology is mechanistically involved in the elevated L-VGCC in CA1 neurons of old 3xTgAD mice.

Our finding of elevated whole-cell L-VGCC in CA1 neurons of old 3xTgAD mice is consistent with considerable previous evidence that excessive Ca^{2+} influx contributes to neuronal degeneration in AD (Bezprozvanny and Mattson, 2008). The lack of an increase in LVGCC in CA3 pyramidal neurons and dentate granule neurons of 3xTgAD mice is consistent with a relative resistance of these neurons to tau pathology in the 3xTgAD mice (Oddo et al., 2003) and to degeneration in AD (Mattson and Magnus, 2006). Studies of other

mouse models of AD support a role for cellular Ca^{2+} overload occurring downstream of Aβ accumulation (Kuchibhotla et al., 2008), and it has been reported that an aberrant elevation of intracellular Ca^{2+} levels in neurons in 3xTgAD mice is partially normalized using nifedipine treatment (Lopez et al., 2008). However, in contrast to the increase in L-VGCC that occurs in CA1 neurons during normal aging (Thibault and Landfield, 1996) and in 3xTgAD mice (present study), it was recently reported that L-VGCC activity in CA1 neurons is reduced in a line of mice expressing mutant amyloid precursor protein and presenilin 1 (Thibault et al., 2012). There are numerous variables in the latter study that differed from the present study including: the electrophysiological recordings were performed in slices from mice that had been subjected to behavioral testing before they were euthanized, whereas our recordings were made from behaviorally naive mice; the background strains of mice are different; the PS1 mutations are different (P264L in the 2xTg mice and M146V in the 3xTgAD mice); and the methods of slice preparation were different (mild enzymatic treatment to partially dissociate cells in area CA1 in Thibault et al., 2012, and conventional slice preparation methods in the present study).

We found that the NMDA current was elevated significantly, albeit modestly, in CA1 neurons of old 3xTgAD mice compared with in age-matched WT mice. Excessive Ca^{2+} influx through NMDA receptor channels is implicated in the neurodegenerative process in AD based on studies in experimental models (Goussakov et al., 2010; Mattson, 2003) and by clinical data demonstrating a disease-modifying effect of the NMDA receptor channel open blocker, memantine, in AD patients (Rogawski and Wenk, 2003). Interestingly, previous studies have suggested that exposure of neurons to Aβ reduces NMDA currents (Snyder et al., 2005), as does expression of mutant PS1 (Wang et al., 2009). In contrast, expression of human tau enhances nonsynaptic NMDA receptor-mediated neuronal degeneration (Amadoro et al., 2006). Because CA1 neurons in 3xTgAD mice express amyloid precursor protein, PS1, and tau mutations, it might be that the human p-tau pathology in CA1 neurons in old 3xTgAD mice is linked mechanistically to the selective elevation of NMDA current in these neurons.

Finally, our findings suggest potential roles for aberrant L-VGCC and NMDA receptor activation in perturbed synaptic plasticity and neuronal network activity in AD. It was previously shown that in-hibitors of L-VGCC can normalize excitability of CA1 neurons in old rats (Moyer et al., 1992; Norris et al., 1998). In addition, disturbances of the ER Ca^{2+} handling might occur in hippocampal neurons during normal aging (Bodhinathan et al., 2010; Kumar and Foster, 2004) and in AD (Bezprozvanny and Mattson, 2008). Moreover, PS1 mutations that cause early-onset inherited AD result in an aberrant release of Ca^{2+} from the ER (Bezprozvanny and Mattson, 2008). Because Ca^{2+} regulation at the plasma and ER membranes are intimately associated, it is reasonable to envision a scenario in which age- and AD-related increases in Ca^{2+} influx via L-VGCC and NMDA receptors enhance ER Ca^{2+} store accumulation and release, thereby perturbing synaptic plasticity and neuronal network activity in ways that impair learning and memory.

Supplementary Material

Refer to Web version on PubMed Central for supplementary material.

Acknowledgments

This research was supported by the Intramural Research Program of the National Institute on Aging of the National Institutes of Health. The authors thank the Comparative Medicine Section of the National Institute on Aging for technical support.

References

Amadoro G, Ciotti MT, Costanzi M, Cestari V, Calissano P, Canu N. NMDA receptor mediates tau-induced neurotoxicity by calpain and ERK/MAPK activation. Proc. Natl. Acad. Sci. U.S.A. 2006; 103:2892–2897. [PubMed: 16477009]

Andrásfalvy BK, Makara JK, Johnston D, Magee JC. Altered synaptic and non-synaptic properties of CA1 pyramidal neurons in Kv4.2 knockout mice. J. Physiol. 2008; 586:3881–3892. [PubMed: 18566000]

Anekonda TS, Quinn JF. Calcium channel blocking as a therapeutic strategy for Alzheimer's disease: the case for isradipine. Biochim. Biophys. Acta. 2011; 1812:1584–1590. [PubMed: 21925266]

Arnold SE, Hyman BT, Flory J, Damasio AR, Van Hoesen GW. The topographical and neuroanatomical distribution of neurofibrillary tangles and neuritic plaques in the cerebral cortex of patients with Alzheimer's disease. Cereb. Cortex. 1991; 1:103–116. [PubMed: 1822725]

Bezprozvanny I, Mattson MP. Neuronal calcium mishandling and the pathogenesis of Alzheimer's disease. Trends Neurosci. 2008; 31:454–463. [PubMed: 18675468]

Bodhinathan K, Kumar A, Foster TC. Intracellular redox state alters NMDA receptor response during aging through Ca2+/calmodulin-dependent protein kinase II. J. Neurosci. 2010; 30:1914–1924. [PubMed: 20130200]

Calderone A, Jover T, Mashiko T, Noh KM, Tanaka H, Bennett MV, Zukin RS. Late calcium EDTA rescues hippocampal CA1 neurons from global ischemia-induced death. J. Neurosci. 2004; 24:9903–9913. [PubMed: 15525775]

Campbell LW, Hao SY, Thibault O, Blalock EM, Landfield PW. Aging changes in voltage-gated calcium currents in hippocampal CA1 neurons. J. Neurosci. 1996; 16:6286–6295. [PubMed: 8815908]

Chakroborty S, Kim J, Schneider C, Jacobson C, Molgó J, Stutzmann GE. Early presynaptic and postsynaptic calcium signaling abnormalities mask underlying synaptic depression in presymptomatic Alzheimer's disease mice. J. Neurosci. 2012; 32:8341–8353. [PubMed: 22699914]

Connor JA, Stevens CE. Voltage clamp studies of a transient outward membrane current in gastropod neural somata. J. Physiol. 1971; 213:21–30. [PubMed: 5575340]

Cottrell DA, Blakely EL, Johnson MA, Ince PG, Turnbull DM. Mitochondrial enzyme-deficient hippocampal neurons and choroidal cells in AD. Neurology. 2001; 57:260–264. [PubMed: 11468310]

Disterhoft JF, Wu WW, Ohno M. Biophysical alterations of hippocampal pyramidal neurons in learning, ageing and Alzheimer's disease. Ageing Res. Rev. 2004; 3:383–406. [PubMed: 15541708]

Flaherty DB, Soria JP, Tomasiewicz HG, Wood JG. Phosphorylation of human tau protein by microtubule-associated kinases: GSK3beta and cdk5 are key participants. J. Neurosci. Res. 2000; 62:463–472. [PubMed: 11054815]

Furukawa K, Wang Y, Yao PJ, Fu W, Mattson MP, Itoyama Y, Onodera H, D'Souza I, Poorkaj PH, Bird TD, Schellenberg GD. Alteration in calcium channel properties is responsible for the neurotoxic action of a familial frontotemporal dementia tau mutation. J. Neurochem. 2003; 87:427–436. [PubMed: 14511120]

Gleichmann M, Chow VW, Mattson MP. Homeostatic disinhibition in the aging brain and Alzheimer's disease. J. Alzheimers Dis. 2011; 24:15–24. [PubMed: 21187584]

Goussakov I, Miller MB, Stutzmann GE. NMDA-mediated Ca (2) influx drives aberrant ryanodine receptor activation in dendrites of young Alzheimer + 's disease mice. J. Neurosci. 2010; 30:12128–12137. [PubMed: 20826675]

Gray JA, Shi Y, Usui H, During MJ, Sakimura K, Nicoll RA. Distinct modes of AMPA receptor suppression at developing synapses by GluN2A and GluN2B: single-cell NMDA receptor subunit deletion in vivo. Neuron. 2011; 71:1085–1101. [PubMed: 21943605]

Guo Q, Fu W, Sopher BL, Miller MW, Ware CB, Martin GM, Mattson MP. Increased vulnerability of hippocampal neurons to excitotoxic necrosis in presenilin-1 mutant knock-in mice. Nat. Med. 1999; 5:101–116. [PubMed: 9883847]

Guo Q, Sopher BL, Furukawa K, Pham DG, Robinson N, Martin GM, Mattson MP. Alzheimer's presenilin mutation sensitizes neural cells to apoptosis induced by trophic factor withdrawal and amyloid beta-peptide: involvement of calcium and oxyradicals. J. Neurosci. 1997; 17:4212–4222. [PubMed: 9151738]

Gustafsson B, Galvan M, Grafe P, Wigstrom H. A transient outward current in a mammalian central neuron blocked by 4-aminopyridine. Nature. 1982; 299:252–254. [PubMed: 6287290]

Halagappa VK, Guo Z, Pearson M, Matsuoka Y, Cutler RG, Laferla FM, Mattson MP. Intermittent fasting and caloric restriction ameliorate age-related behavioral deficits in the triple-transgenic mouse model of Alzheimer's disease. Neurobiol. Dis. 2007; 26:212–220. [PubMed: 17306982]

Ito E, Oka K, Etcheberrigaray R, Nelson TJ, McPhie DL, Tofel-Grehl B, Gibson GE, Alkon DL. Internal Ca2+ mobilization is altered in fibroblasts from patients with Alzheimer disease. Proc. Natl. Acad. Sci. U.S.A. 1994; 91:534–538. [PubMed: 8290560]

Kashiwaya Y, Bergman C, Lee JH, Wan R, King MT, Mughal MR, Okun E, Clarke K, Mattson MP, Veech RL. Ketone ester diet exhibits anxiolytic and cognition-sparing properties, and lessens amyloid and tau pathologies in a mouse model of Alzheimer's disease. Neurobiol. Aging. 2013; 34:1530–1539. [PubMed: 23276384]

Kawas CH, Corrada MM. Alzheimer's and dementia in the oldest-old: a century of challenges. Curr. Alzheimers Res. 2006; 3:411–419.

Kochlamazashvili G, Henneberger C, Bukalo O, Dvoretskova E, Senkov O, Lievens PM, Westenbroek R, Engel AK, Catterall WA, Rusakov DA, Schachner M, Dityatev A. The extracellular matrix molecule hyaluronic acid regulates hippocampal synaptic plasticity by modulating postsynaptic L-type Ca(2+) channels. Neuron. 2010; 67:116–128. [PubMed: 20624596]

Kuchibhotla KV, Goldman ST, Lattarulo CR, Wu HY, Hyman BT, Bacskai BJ. Aβ plaques lead to aberrant regulation of calcium homeostasis in vivo resulting in structural and functional disruption of neuronal networks. Neuron. 2008; 59:214–225. [PubMed: 18667150]

Kumar A, Foster TC. Enhanced long-term potentiation during aging is masked by processes involving intracellular calcium stores. J. Neurophysiol. 2004; 91:2437–2444. [PubMed: 14762159]

Landfield PW. Increased hippocampal Ca2+ channel activity in brain aging and dementia. Hormonal and pharmacologic modulation. Ann. N. Y. Acad. Sci. 1994; 747:351–364. [PubMed: 7847683]

Landfield PW, Campbell LW, Hao SY, Kerr DS. Aging-related increases in voltage-sensitive, inactivating calcium currents in rat hippocampus. Implications for mechanisms of brain aging and Alzheimer's disease. Ann. N. Y. Acad. Sci. 1989; 568:95–105. [PubMed: 2560904]

Larner AJ. Epileptic seizures in AD patients. Neuromolecular Med. 2011; 12:71–77. [PubMed: 19557550]

Levere TE, Walker A. Old age and cognition: enhancement of recent memory in aged rats by the calcium channel blocker nimodipine. Neurobiol. Aging. 1992; 13:63–66. [PubMed: 1542383]

Liu D, Pitta M, Lee JH, Ray B, Lahiri DK, Furukawa K, Mughal M, Jiang H, Villarreal J, Cutler RG, Greig NH, Mattson MP. The KATP channel activator diazoxide ameliorates amyloid-b and tau pathologies and improves memory in the 3xTgAD mouse model of Alzheimer's disease. J. Alzheimers Dis. 2010; 22:443–457. [PubMed: 20847430]

Lopez JR, Lyckman A, Oddo S, Laferla FM, Querfurth HW, Shtifman A. Increased intraneuronal resting [Ca2+] in adult Alzheimer's disease mice. J. Neurochem. 2008; 105:262–271. [PubMed: 18021291]

Lu W, Gray JA, Granger AJ, During MJ, Nicoll RA. Potentiation of synaptic AMPA receptors induced by the deletion of NMDA receptors requires the GluA2 subunit. J. Neurophysiol. 2011; 105:923–928. [PubMed: 20980546]

Mark RJ, Hensley K, Butterfield DA, Mattson MP. Amyloid beta-peptide impairs ion-motive ATPase activities: evidence for a role in loss of neuronal Ca2+ homeostasis and cell death. J. Neurosci. 1995; 15:6239–6249. [PubMed: 7666206]

Mark RJ, Pang Z, Geddes JW, Uchida K, Mattson MP. Amyloid beta-peptide impairs glucose transport in hippocampal and cortical neurons: involvement of membrane lipid peroxidation. J. Neurosci. 1997; 17:1046–1054. [PubMed: 8994059]

Matthews EA, Linardakis JM, Disterhoft JF. The fast and slow after-hyperpolarizations are differentially modulated in hippocampal neurons by aging and learning. J. Neurosci. 2009; 29:4750–4755. [PubMed: 19369544]

Mattson MP. Antigenic changes similar to those seen in neurofibrillary tangles are elicited by glutamate and Ca2+ in flux in cultured hippocampal neurons. Neuron. 1990; 4:105–117. [PubMed: 1690014]

Mattson MP. Excitotoxic and excitoprotective mechanisms: abundant targets for the prevention and treatment of neurodegenerative disorders. Neuromolecular Med. 2003; 3:65–94. [PubMed: 12728191]

Mattson MP, Cheng B, Davis D, Bryant K, Lieberburg I, Rydel RE. Beta-amyloid peptides destabilize calcium homeostasis and render human cortical neurons vulnerable to excitotoxicity. J. Neurosci. 1992; 12:376–389. [PubMed: 1346802]

Mattson MP, Magnus T. Ageing and neuronal vulnerability. Nat. Rev. Neurosci. 2006; 7:278–294. [PubMed: 16552414]

Medeiros R, Kitazawa M, Chabrier MA, Cheng D, Baglietto-Vargas D, Kling A, Moeller A, Green KN, LaFerla FM. Calpain inhibitor A-705253 mitigates Alzheimer's disease-like pathology and cognitive decline in aged 3xTgAD mice. Am. J. Pathol. 2012; 181:616–625. [PubMed: 22688056]

Moyer JR, Thompson LT, Black JP, Disterhoft JF. Nimodipine increases excitability of rabbit CA1 pyramidal neurons in an age- and concentration-dependent manner. J. Neurophysiol. 1992; 68:2100–2109. [PubMed: 1491260]

Norris CM, Halpain S, Foster TC. Reversal of age-related alterations in synaptic plasticity by blockade of L-type Ca2+ channels. J. Neurosci. 1998; 18:3171–3179. [PubMed: 9547225]

Oddo S, Caccamo A, Shepherd JD, Murphy MP, Golde TE, Kayed R, Metherate R, Mattson MP, Akbari Y, LaFerla FM. Triple-transgenic model of Alzheimer's disease with plaques and tangles: intracellular Abeta and synaptic dysfunction. Neuron. 2003; 39:409–421. [PubMed: 12895417]

Oulès B, Del Prete D, Greco B, Zhang X, Lauritzen I, Sevalle J, Moreno S, Paterlini-Bréchot P, Trebak M, Checler F, Benfenati F, Chami M. Ryanodine receptor blockade reduces amyloid-b load and memory impairments in Tg2576 mouse model of Alzheimer disease. J. Neurosci. 2012; 32:11820–11834. [PubMed: 22915123]

Paris D, Bachmeier C, Patel N, Quadros A, Volmar CH, Laporte V, Ganey J, Beaulieu-Abdelahad D, Ait-Ghezala G, Crawford F, Mullan MJ. Selective antihypertensive dihydropyridines lower Aβ accumulation by targeting both the production and the clearance of Aβ across the blood-brain barrier. Mol. Med. 2011; 17:149–162. [PubMed: 21170472]

Peng J, Liang G, Inan S, Wu Z, Joseph DJ, Meng Q, Peng Y, Eckenhoff MF, Wei H. Dantrolene ameliorates cognitive decline and neuropathology in Alzheimer triple transgenic mice. Neurosci. Lett. 2012; 516:274–279. [PubMed: 22516463]

Porter NM, Thibault O, Thibault V, Chen KC, Landfield PW. Calcium channel density and hippocampal cell death with age in long-term culture. J. Neurosci. 1997; 17:5629–5639. [PubMed: 9204944]

Roberts-Lewis JM, Savage MJ, Marcy VR, Pinsker LR, Siman R. Immunolocalization of calpain I-mediated spectrin degradation to vulnerable neurons in the ischemic gerbil brain. J. Neurosci. 1994; 14:3934–3944. [PubMed: 8207497]

Rogawski MA, Wenk GL. The neuropharmacological basis for the use of memantine in the treatment of Alzheimer's disease. CNS Drug Rev. 2003; 9:275–308. [PubMed: 14530799]

Saito K, Elce JS, Hamos JE, Nixon RA. Widespread activation of calcium-activated neutral proteinase (calpain) in the brain in Alzheimer disease: a potential molecular basis for neuronal degeneration. Proc. Natl. Acad. Sci. U.S.A. 1993; 90:2628–2632. [PubMed: 8464868]

Sandin M, Jasmin S, Levere TE. Aging and cognition: facilitation of recent memory in aged nonhuman primates by nimodipine. Neurobiol. Aging. 1990; 11:573–575. [PubMed: 2234289]

Santos SF, Pierrot N, Octave JN. Network excitability dysfunction in Alzheimer's disease: insights from in vitro and in vivo models. Rev. Neurosci. 2010; 21:153–171. [PubMed: 20879690]

Schaefer AT, Helmstaedter M, Sakmann B, Korngreen A. Correction of conductance measurements in non-space-clamped structures: 1. Voltage-gated K+ channels. Biophys. J. 2003; 84:3508–3528. [PubMed: 12770864]

Schellenberg GD, Montine TJ. The genetics and neuropathology of Alzheimer's disease. Acta Neuropathol. 2012; 124:305–323. [PubMed: 22618995]

Schoppa NE, Kinzie JM, Sahara Y, Segerson TP, Westbrook GL. Den-drodendritic inhibition in the olfactory bulb is driven by NMDA receptors. J. Neurosci. 1998; 18:6790–6802. [PubMed: 9712650]

Shankar GM, Bloodgood BL, Townsend M, Walsh DM, Selkoe DJ, Sabatini BL. Natural oligomers of the Alzheimer amyloid-beta protein induce reversible synapse loss by modulating an NMDA-type glutamate receptor-dependent signaling pathway. J. Neurosci. 2007; 27:2866–2875. [PubMed: 17360908]

Simonian NA, Hyman BT. Functional alterations in neural circuits in Alzheimer's disease. Neurobiol. Aging. 1995; 16:305–309. [PubMed: 7566339]

Snyder EM, Nong Y, Almeida CG, Paul S, Moran T, Choi EY, Nairn AC, Salter MW, Lombroso PJ, Gouras GK, Greengard P. Regulation of NMDA receptor trafficking by amyloid-beta. Nat. Neurosci. 2005; 8:1051–1058. [PubMed: 16025111]

Storm JF. Potassium currents in hippocampal pyramidal cells. Prog. Brain Res. 1990; 83:161–187. [PubMed: 2203097]

Stuart GJ, Sakmann B. Active propagation of somatic action potentials into neocortical pyramidal cell dendrites. Nature. 1994; 367:69–72. [PubMed: 8107777]

Thibault O, Landfield PW. Increase in single L-type calcium channels in hippocampal neurons during aging. Science. 1996; 272:1017–1020. [PubMed: 8638124]

Thibault O, Pancani T, Landfield PW, Norris CM. Reduction in neuronal L-type calcium channel activity in a double knock-in mouse model of Alzheimer's disease. Biochim. Biophys. Acta. 2012; 1822:546–549. [PubMed: 22265986]

Veng LM, Mesches MH, Browning MD. Age-related working memory impairment is correlated with increases in the L-type calcium channel protein alpha1D (Cav1.3) in area CA1 of the hippocampus and both are ameliorated by chronic nimodipine treatment. Mol. Brain. Res. 2003; 110:193–202. [PubMed: 12591156]

Wang Y, Greig NH, Yu QS, Mattson MP. Presenilin-1 mutation impairs cholinergic modulation of synaptic plasticity and suppresses NMDA currents in hippocampus slices. Neurobiol. Aging. 2009; 30:1061–1068. [PubMed: 18068871]

Wu HY, Hudry E, Hashimoto T, Kuchibhotla K, Rozkalne A, Fan Z, Spires-Jones T, Xie H, Arbel-Ornath M, Grosskreutz CL, Bacskai BJ, Hyman BT. Amyloid beta induces the morphological neurodegenerative triad of spine loss, dendritic simplification, and neuritic dystrophies through calcineurin activation. J. Neurosci. 2010; 30:2636–2649. [PubMed: 20164348]

Yagami T, Ueda K, Sakaeda T, Itoh N, Sakaguchi G, Okamura N, Hori Y, Fujimoto M. Protective effects of a selective L-type voltage-sensitive calcium channel blocker, S-312-d, on neuronal cell death. Biochem. Pharmacol. 2004; 67:1153–1165. [PubMed: 15006551]

Yao J, Irwin RW, Zhao L, Nilsen J, Hamilton RT, Brinton RD. Mitochondrial bioenergetic deficit precedes Alzheimer's pathology in female mouse model of Alzheimer's disease. Proc. Natl. Acad. Sci. U.S.A. 2009; 106:14670–14675. [PubMed: 19667196]

Zhang J, Wang Y, Chi Z, Keuss MJ, Pai YM, Kang HC, Shin JH, Bugayenko A, Wang H, Xiong Y, Pletnikov MV, Mattson MP, Dawson TM, Dawson VL. Thorase, a novel AAA+ ATPase, regulates AMPA receptor-dependent synaptic plasticity and behavior. Cell. 2011; 145:284–299. [PubMed: 21496646]

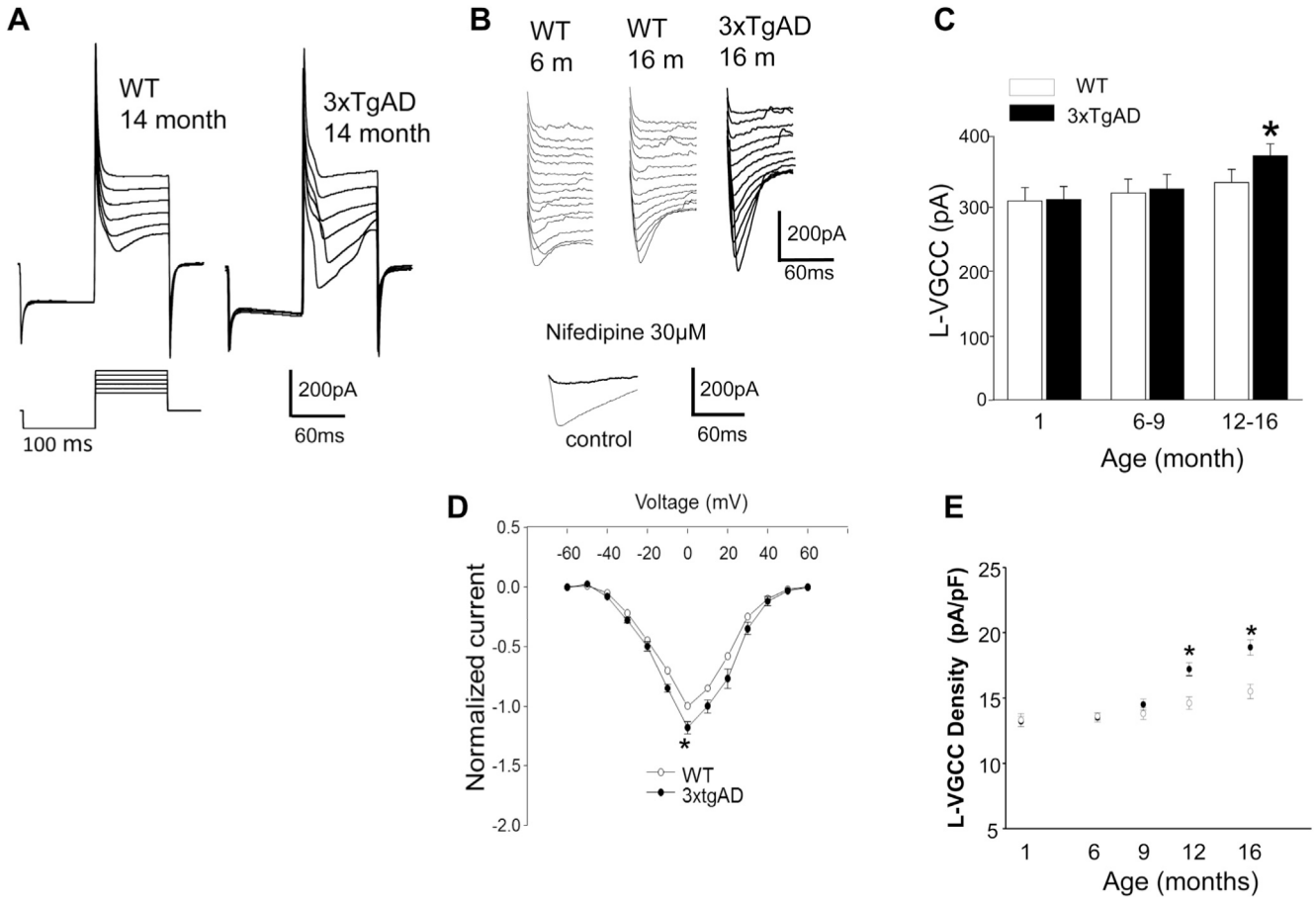

Fig. 1.

Whole-cell L-VGCC amplitude and density is elevated, in an age-dependent manner, in CA1 hippocampal neurons of 3xTgAD mice compared with in WT mice. (A) Representative current traces and protocol for recording of L-VGCCs. Command depolarizing steps to 40 mV, in 20-mV steps, after a 100-ms hyperpolarizing step to −100 mV from a holding potential of −60 mV. Recordings are from hippocampal slices from 14-month-old WT and 3xTgAD mice. (B) The L-VGCC is elevated in old 3xTgAD mice compared with in WT mice. Upper panel, representative traces from CA1 neurons in slices from WT and 3xTgAD mice of the indicated ages, the voltage steps are 10 mV. Lower panel, traces showing that the Ca^{2+} current is completely blocked by the L-type channel blocker nifedipine. (C) Histogram of averaged CA1 L-VGCC in hippocampal slices from WT and 3xTgAD mice of the indicated ages (mean ± standard error of the mean; $n = 6$ mice per group with recordings made from a total of 6–12 neurons). * $p < 0.05$. (D) IV curves for recordings from CA1 neurons from 12–16-month-old WT and 3xTgAD mice. (E) Plot of L-VGCC current density (peak whole-cell current divided by the cell capacitance) plotted as a function of age in CA1 neurons of WT and 3xTgAD mice. * $p < 0.05$ compared with the WT value. Abbreviations: L-VGCC, L-type Ca^{2+} current; WT, wild type; IV, current/voltage.

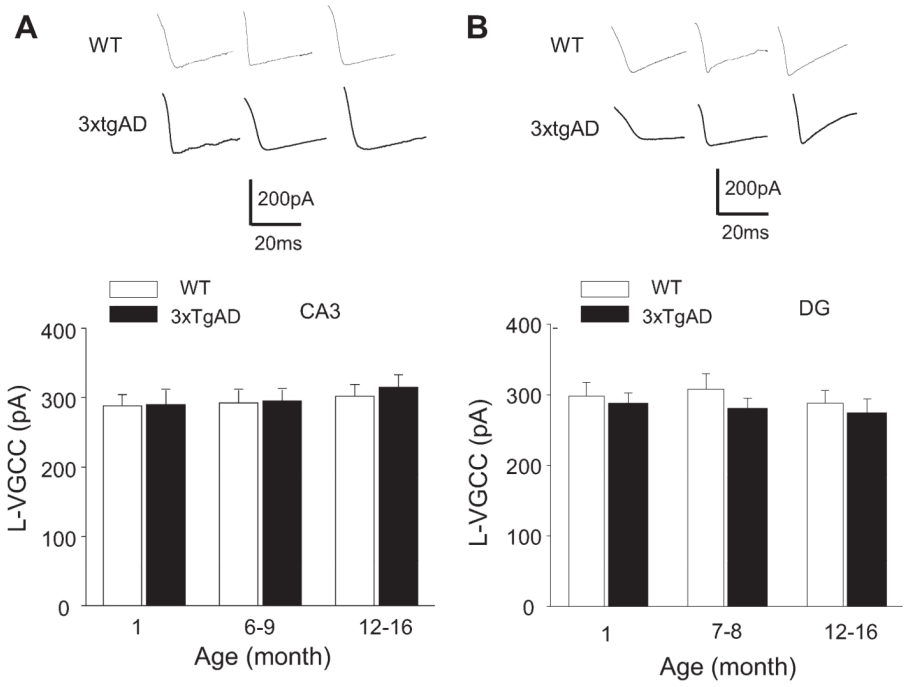

Fig. 2.

L-VGCC in CA3 and dentate granule neurons are unaltered in 3xTgAD mice. (A) Top, representative traces of L-VGCC in CA3 neurons in WT and 3xTgAD mice of the indicated ages. Bottom, levels of L-VGCC in CA3 neurons in WT and 3xTgAD mice of the indicated ages. Values are the mean and standard error of the mean (n = 5–8 neurons in slices from 4–6 mice). (B) Top, representative traces of L-VGCC in dentate granule neurons in WT and 3xTgAD mice of the indicated ages. Bottom, levels of L-VGCC in dentate granule neurons in WT and 3xTgAD mice of the indicated ages. Values are the mean and standard error of the mean (n = 5–8 neurons in slices from 4–6 mice). Abbreviations: L-VGCC, L-type Ca^{2+} current; WT, wild type.

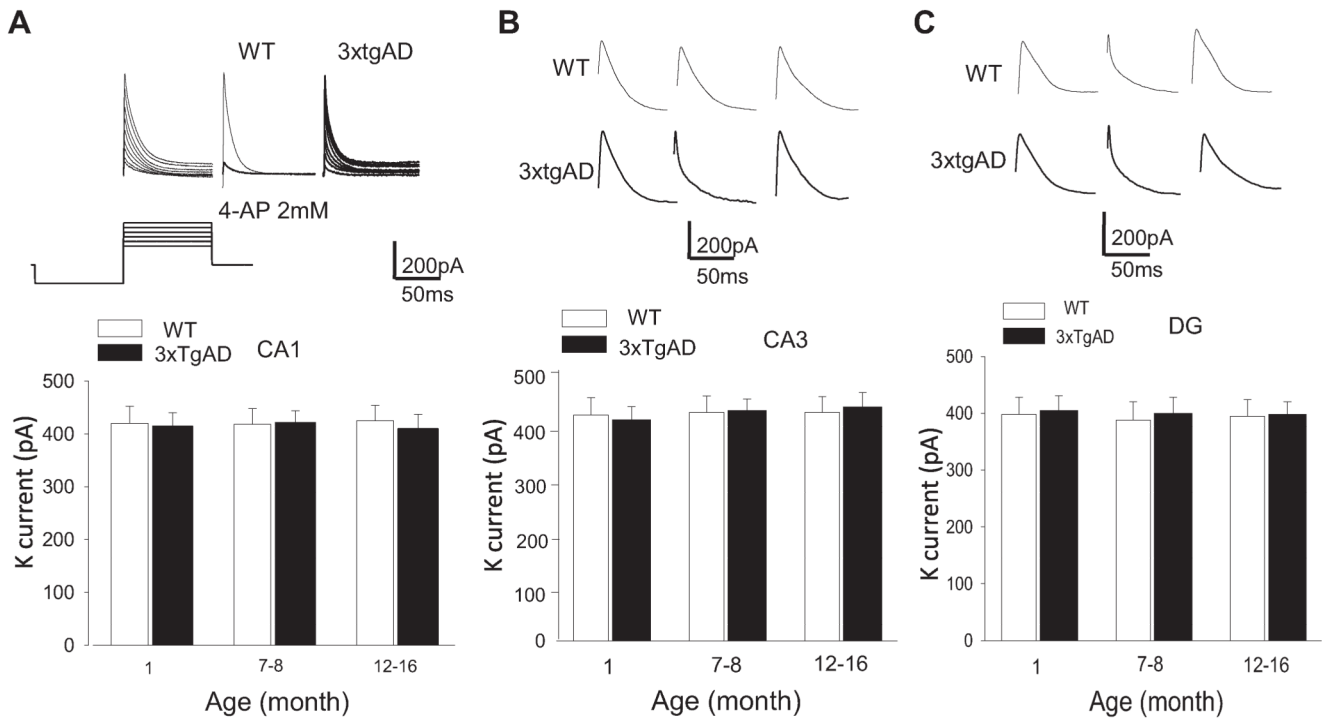

Fig. 3.

The 4–AP-sensitive K^+ channel current in CA1 neurons is unaltered by aging and in 3xTgAD mice. (A) The upper panels show representative traces of K^+ currents recorded in CA1 neurons from WT mice at steps from 40 mV to −70 mV (left) or only at 40 mV (middle), and in a slice treated with 2 mM 4-AP (right); at the bottom is the induction protocol. The lower graph shows the results of measurements of K^+ currents in CA1 neurons in WT and 3xTgAD mice of the indicated ages. Values are the mean and standard error of the mean (n = 5–8 neurons in slices from 4–6 mice). (B) and (C) Top, representative traces of K^+ currents in CA3 neurons (B) and dentate granule neurons (C) in WT and 3xTgAD mice of the indicated ages. Bottom, levels of K^+ currents in CA3 neurons (B) and dentate granule neurons (C) in WT and 3xTgAD mice of the indicated ages. Values are the mean and standard error of the mean (n = 5–8 neurons in slices from 4–6 mice). Abbreviations: AP, aminopyridine; WT, wild type.

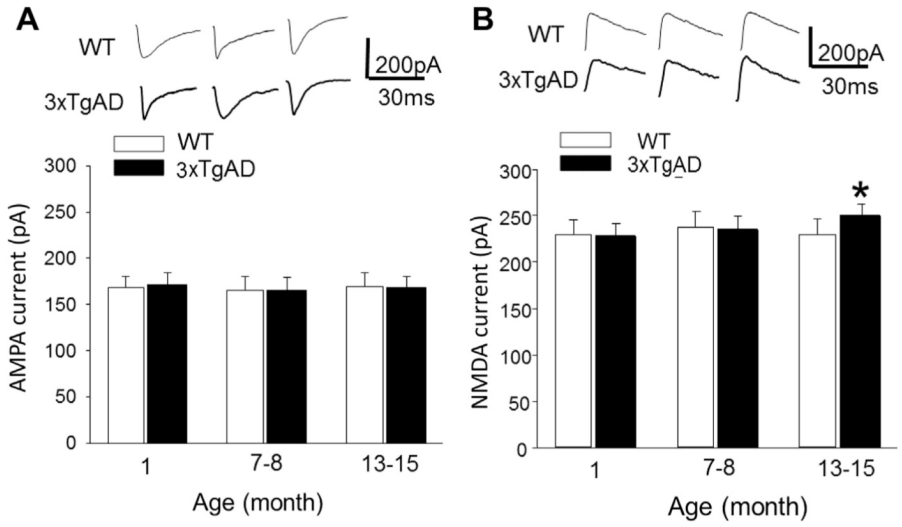

Fig. 4.

NMDA current amplitude is elevated in old 3xTgAD mice. (A) AMPA currents in CA1 neurons in slices from WT and 3xTgAD mice of the indicated ages. (B) NMDA currents in CA1 neurons in slices from WT and 3xTgAD mice of the indicated ages. * $p < 0.05$. Values are the mean and standard error of the mean (n = 5–8 neurons in slices from 4–6 mice). Abbreviations: AMPA, 2-amino-3-(3-hydroxy-5-methyl-isoxazol-4-yl)propanoic acid; NMDA, N-methyl-D-aspartate; WT, wild type.